IOP Conf. Series: Journal of Physics: Conf. Series **1474** (2020) 012018 doi:10.1088/1742-6596/1474/1/012018

Analytical prediction of thermal stresses in composite shells

A Janakiraman[1], R Velmurugan[2*], R Jayaganthan[2], and G Rajasingh[3]

[1]Technical University of Munich Asia, Singapore
[2]Department of Aerospace Engineering, IIT Madras, India
[3]Defence Research and Development Laboratory, Hyderabad, India

E-mail: *ramanv@iitm.ac.in

Abstract. The use of fibre-reinforced plastics or FRPs in various industries, such as aviation, automobiles, renewable energy, etc. has drastically increased over the past decades, owing to the significant strength to weight ratios they offer. The design phase of such components must also factor in thermal loads. Thermal expansions and contractions, when restricted, lead to the buildup of stresses in a material. The distribution of these stresses across the layers of a composite tube has been dealt with here with the help of an analytical study, taking into account any radially varying user-defined temperature profile. On account of geometry, the cases handled are axisymmetric and therefore, shear stresses aren't considered.

1. Introduction

Fibre reinforced polymers are a class of composite materials comprising of two parts: the fibre reinforcement that carries most of the load, and a polymer matrix that binds the fibres together and aids in load transfer from one fibre to another. The presence of reinforcement is to improve the load carrying capacity of the material along the fibre direction; that is to say, the resultant material is anisotropic in nature.

Traditional isotropic materials such as steel and aluminium are being swapped with composite materials, owing to the possibility of property tailoring that the latter allow. Construction of parts using composites is done by laying up several anisotropic composite laminae, which consequently allows us to fortify a component with a greater stiffness along a load path. Thus, by reducing the strengths along the less critical directions, significant weight reductions can be realized. This advantage however, increases the complexity of design, as it becomes important to consider the effects that stacking has on the part's net properties, as well as the variation of parameters such as strain and stress across the different layers of the laminate.

The design of cylindrical components, such as those used in pressure vessels, additionally involves thermal loads in the analysis. Thermal loads may manifest as temperature variations along any of the three directions, and may be static or dynamic. It is however, convenient to analyze static loading in cases where the loads are known to be more or less constant. Axisymmetric plane-strain conditions in a problem further simplify the analysis, whereby the variations along the $\theta-$ and $z-$ directions may be safely neglected. However, the complexity of calculation persists despite these assumptions, as numerous iterations are to be performed to obtain a displacement solution for each radial position. Moreover, stiffness matrices and other

property matrices/vectors become unwieldly as the number of laminae/fibre orientations in the laminate increase. Temperature variations, although limited to the radial direction, may be linear or non-linear and further add to the complexity of calculations.

Cylindrical components consisting of composite laminates, whose laminae are oriented in different directions, are subjected to thermal stresses even when not constrained at the ends, because of varying stiffness values and in some cases, varying coefficients of thermal expansion (CTE) across the layers. The tendency for one layer to expand or contract may be opposed by an adjacent layer with opposite tendencies. For instance, graphite/epoxy laminae have negative CTEs in their axial directions and positive CTEs in the transverse direction. Therefore, an increase or decrease in temperature in a [0/90] layup will result in internal stresses in the laminate, and even bending.

Therefore, it is desirable to prescribe a model through a set of steps to handle these complexities, and is accomplished through analytical studies. The work done in [1] provides a foundation for such an analysis. To analyze these stresses, shell-element approaches have been implemented before in [2–4]. Higher order shell theories may help to better predict, variations of stresses and displacements through the thickness. However, the elasticity approach, which has been implemented in this work, seemed to be more comprehensive. The isotropic case dealt with must be carefully extrapolated to an anisotropic case, as has been done in [5–7]. The present study will therefore base itself on the parameters involved in the derivations. Validation of the same shall be done using values from existing literature and the corresponding results.

2. Formulation

We may describe the stress-strain relationship for a composite material to be,

$$\sigma_{ij} = Q_{ij}(\varepsilon_{ij} - \alpha_{ij}T) \tag{1}$$

where σ is stress (N/m^2), Q is stiffness (N/m^2), ε is strain, α is coefficient of thermal expansion (1/°C), T is temperature change (°C). Converting equation (1) into cylindrical co-ordinates as has been done in [8] gives us,

$$\begin{pmatrix} \varepsilon_r \\ \varepsilon_\theta \\ \varepsilon_z \\ \gamma_{\theta z} \\ \gamma_{rz} \\ \gamma_{r\theta} \end{pmatrix} - \begin{pmatrix} \alpha_r \\ \alpha_\theta \\ \alpha_z \\ 0 \\ 0 \\ 0 \end{pmatrix} T = \begin{pmatrix} \bar{S}_{33} & \bar{S}_{32} & \bar{S}_{31} & \bar{S}_{36} & 0 & 0 \\ & \bar{S}_{22} & \bar{S}_{21} & \bar{S}_{26} & 0 & 0 \\ & & \bar{S}_{11} & \bar{S}_{16} & 0 & 0 \\ & & & \bar{S}_{66} & 0 & 0 \\ & \text{sym} & & & \bar{S}_{55} & \bar{S}_{54} \\ & & & & & \bar{S}_{44} \end{pmatrix} \begin{pmatrix} \sigma_r \\ \sigma_\theta \\ \sigma_z \\ \tau_{\theta z} \\ \tau_{rz} \\ \tau_{r\theta} \end{pmatrix}, \tag{2}$$

where the $\bar{S}_{ij}$ terms represent the values in the transformed compliance matrix.

Considering an axisymmetric problem (radial temperature distribution), we may equate shear strains to zero. Let us allow the axial strain $\varepsilon_z = \partial w/\partial z = \varepsilon_o$. Furthermore, the strain displacement relations in cylindrical co-ordinates are,

$$\varepsilon_r = \frac{\partial u(r)}{\partial r}, \tag{3}$$

$$\varepsilon_\theta = \frac{u(r)}{r}, \tag{4}$$

where $u(r)$ represents the displacement function. Inverting equation (2) and substituting equations (3) and (4) into the same, we get the stress-displacement relations. These relations must consequently satisfy the equilibrium relation in cylindrical co-ordinates,

$$\frac{\partial \sigma_r}{\partial r} + \frac{\sigma_r - \sigma_\theta}{r} = 0. \tag{5}$$

Substituting the expressions for σ_r and σ_θ and solving the equation gives the general expression for displacement as,

$$u(r) = k_1 r^2 + k_2 r + C_1 r^{k_3} + \frac{C_2}{r^{k_4}} + k_5 \varepsilon_o r \tag{6}$$

where k_1, k_2, k_3, k_4, and k_5 are consequences of material and geometric data, and C_1 and C_2 are constants of integration. All constants assume different values for different layers. Therefore, for a layup containing n laminae, we obtain n unique solutions and $2n$ integration constants (C_1 to C_{2n}). At the inner (r_i) and outermost (r_o) layers, if the pressure differential across the entire laminate is zero,

$$\sigma_r^1(r_\mathrm{i}) = 0, \tag{7}$$
$$\sigma_r^n(r_\mathrm{o}) = 0. \tag{8}$$

Moreover, continuity of displacement and strain necessitate that,

$$u_r^p(r_q) = u_r^{p+1}(r_q), \tag{9}$$
$$\left.\frac{\partial u_r^p(r)}{\partial r}\right|_{r=r_q} = \left.\frac{\partial u_r^{p+1}(r)}{\partial r}\right|_{r=r_q}, \tag{10}$$

This means to say that the displacements and radial strains of two adjacent layers are equal at their interface. A layup with n layers will have $(n-1)$ interfaces, and hence we have $2(n-1)$ equations from these conditions. Including equations (7) and (8), we get a total of $2n$ equations for the $2n$ integrations constants we have, allowing us to obtain valid solutions for each layer.

For a fully constrained cylinder, $\varepsilon_o = 0$. At the ends of the cylinder, we must take care of the axial forces. Since all forces are internal,

$$\sum_{i=1}^{n} \int_{r_i}^{r_{i+1}} 2\pi r \sigma_z \, dr = 0, \tag{11}$$

from which we may obtain the value of ε_o if the problem does not involve plane strain. Thus having obtained $u(r)$ for each layer, we may obtain stresses and strains across the laminate.

3. Materials and methods

To obtain the variation of mechanical properties with temperature, GFRP specimens for different tests were prepared. Glass fibre plates of size 290×290 mm were prepared using glass fibre mats (figure 1). The epoxy used was prepared by mixing Araldite LY556 resin with HY995 hardener in the weight ratio of 10 : 1. Hand layup technique was implemented, and the layup was subjected to a temperature of 70°C and pressure of 10 bar. The heater was switched off after half an hour, and the pressure released after 4 hours. Finally, a post-curing time of 24 hours was allowed before cutting the plate into test specimens. A fibre volume fraction of about 53% was achieved.

3.1. Tensile test

Specimens were cut and tests were performed adhering to guidelines provided by ASTM D3039. In order to measure the Poisson's ratio, the Digital Image Correlation (DIC) method was implemented, whereby the samples were coated with a layer of white paint, on top of which a random pattern of black dots was added. The 0° specimens are similar to the one shown in figure 2.

Tests were performed at room temperature (33°C), 60, 70, 80, and 90°C, with at least three specimens being tested at each temperature. For this, a Universal Testing Machine (UTM) with

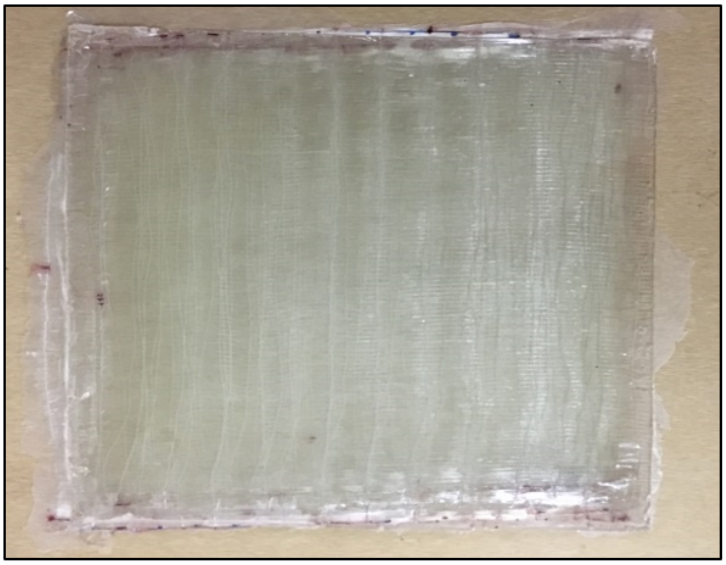

Figure 1. GFRP plate

Figure 2. Tensile Test specimen — 0° fibre orientation

a provision for an oven was used. Each specimen was mounted onto the UTM, and the oven temperature set to the required value. The specimen to be tested was allowed to soak for at least half an hour at the set temperature before the test commenced. Modulus values were obtained from the Load-Displacement curves generated.

Images for DIC were recorded by a camera capable of a maximum frame rate of 15 frames/s (figure 3). However, only one image was saved per second of recording, to remove redundancy and save on processing time. The correlation itself was done using the DIC software, Vic2D. The strains generated thereby were used to calculate the Poisson's ratio of each specimen. The above procedure was repeated for the 90° samples, except DIC, since the Poisson's ratio ν_{21} can be calculated using ν_{12}, E_1, and E_2.

3.2. Dilatometry

To obtain the coefficients of thermal expansion (CTE) α_1 and α_2, dilatometry was performed. A dilatometer supplied by VB Ceramics, Chennai was used. Specimens of dimensions 40×10 mm were prepared and the tests were performed between 33 and 90°C. Recordings were made for every 1°C rise in temperature, and the corresponding CTE at each temperature was automatically computed.

The results from the aforementioned tests were then plotted. Curve fitting was implemented, so that the variations may be used in the analytical model developed.

4. Results and Discussion

The present work is verified in section 4.1 by adopting the problem dealt with in [9].

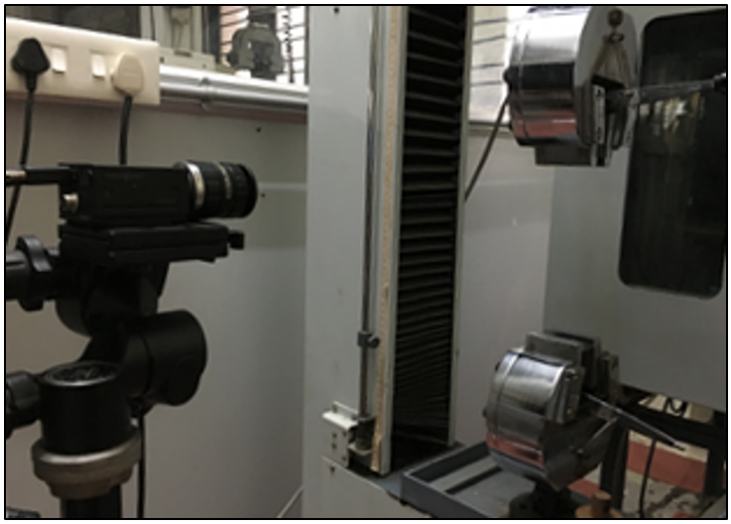

Figure 3. Setup for image capture

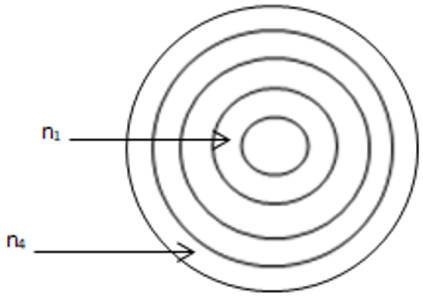

Figure 4. Cross-section of the composite cylinder with a $[0/90]_2$

Table 1. Mechanical properties of the graphite-epoxy 0° laminae.

Fibre	Moduli ($10^9\,\mathrm{N/m^2}$)						CTE ($10^{-6}/°\mathrm{C}$)		
direction	E_1	E_2	E_3	ν_{12}	ν_{23}	ν_{13}	α_1	α_2	α_3
Axial	146.8	9.929	9.101	0.3956	0.0157	0.3127	−0.0774	33.66	33.66

4.1. Verification

A cylinder with an orthotropic laminate is allowed to deform in space, where the temperature is 280°C below the laminate's curing temperature of about 150°C. A schematic of the problem is depicted in figure 4.

The inner radius of the cylinder was 6.35 mm, and the individual layer thicknesses were 0.127 mm each. The layup of the laminate comprised of alternating 0° and 90° laminae, and consisted of 4 layers in total. The temperature of the cylinder was uniform throughout, and maintained at around −130°C. Deformation was allowed to occur without any end constraints. The mechanical properties of the 0° are listed in table 1.

As done earlier, the results from the original work and the present study are juxtaposed below in figure 5.

Figure 5*a* depicts the axial stress variation through the thickness of the cylinder. As can

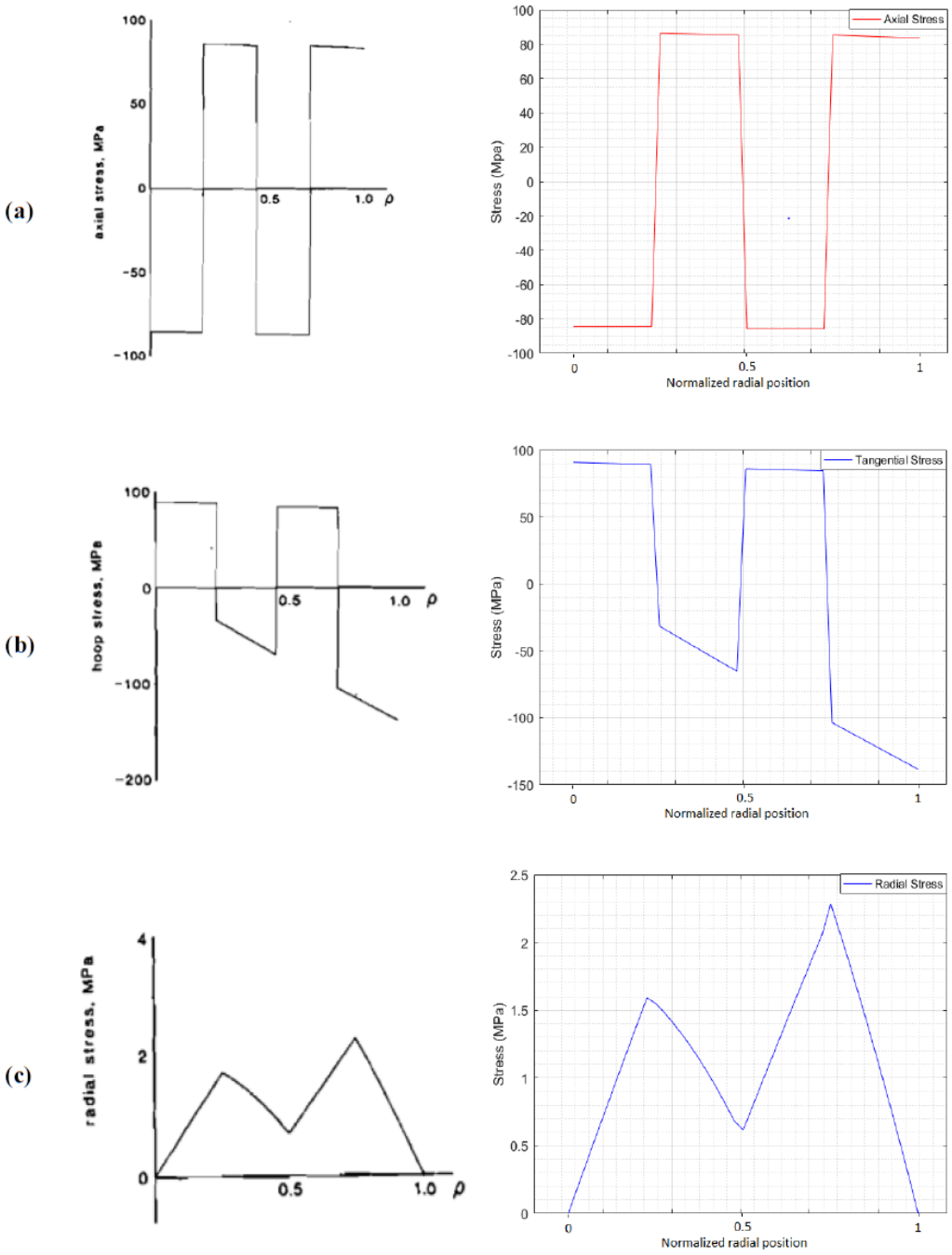

Figure 5. Comparison of results: axial stress (a), hoop stress (b), radial stress (c). Courtesy of images on the left: [9]

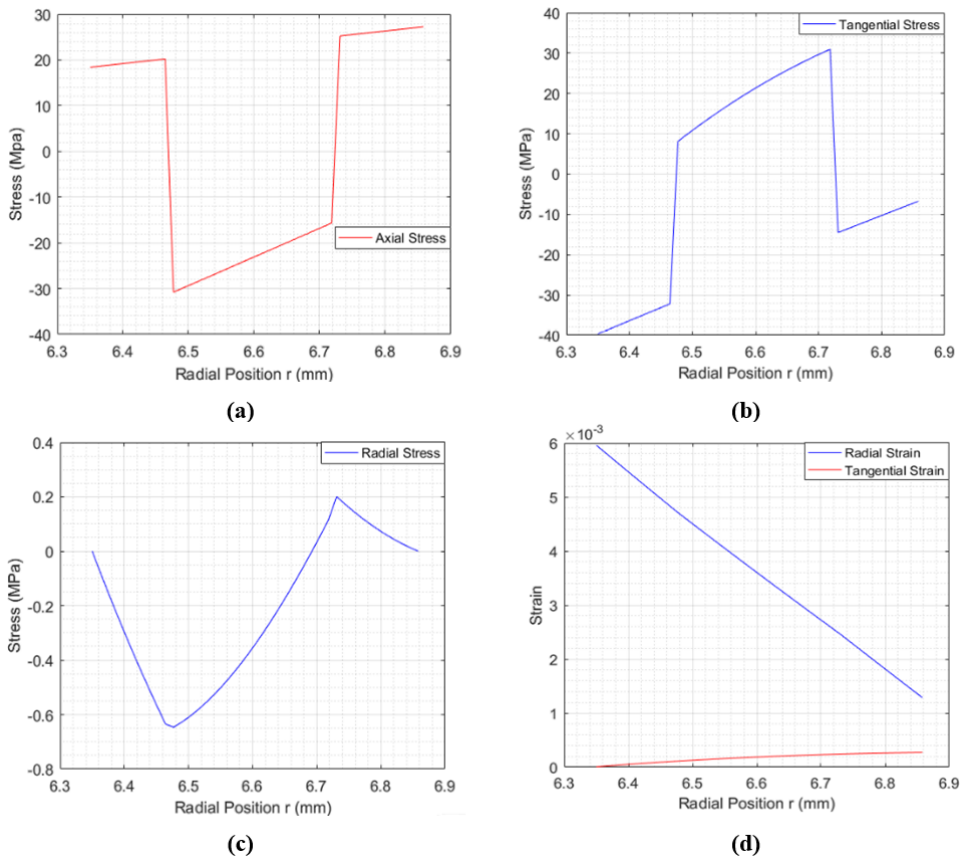

Figure 6. Variations of axial stress (a), hoop stress (b), radial stress (c), radial and hoop strain (d) in a $[0/90]_s$ layup

be seen, there is good accordance with the results from the original work. The tendency for the 0° layers to expand as the temperature drops (due to a negative CTE) is restricted by the opposite tendency for the 90° layers to contract. Thus, along the axial direction, the 0° layers are subjected to a compressive stress, while the 90° layers, a tensile stress.

Figures 5b and 5c depict the hoop stress and radial stress variations, which also conform well to the results of the original work. The hoop stresses for the 0° layers are tensile because their CTEs are positive in the hoop/tangential direction. A similar argument may be put forth for the 90° layers.

This study extends itself into section 4.2, with an example that shows the variations of stresses and strains in cylindrical shell with a $[0/90]_s$ layup. The material properties used are listed in table 1. The temperature on the inner surface is maintained at 120°C, while that on the outer surface is 30°C. The variation of temperature here is linear, but any user defined variation may be substituted for T.

4.2. Layup: $[0/90]_s$

From figure 6a, we see that the axial stress is tensile in nature in the 0° laminae and compressive in the 90° laminae. Within the 0° laminae, the tensile stress increases as we move radially outward; a similar shift towards a tensile regime is visible within the 90° laminae as well.

The variations in stress may be explained by the existence of bending moments. The innermost lamina (0°) maintained at 120°C, due to its negative CTE, will tend to contract,

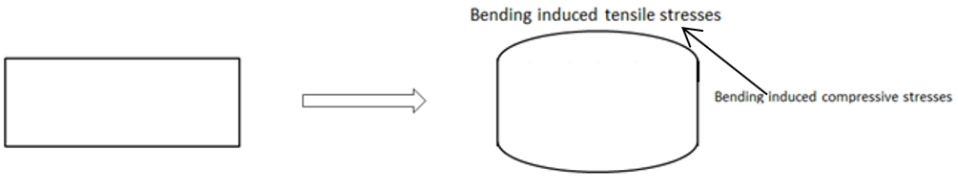

Figure 7. Exaggerated schematic showing possible bending

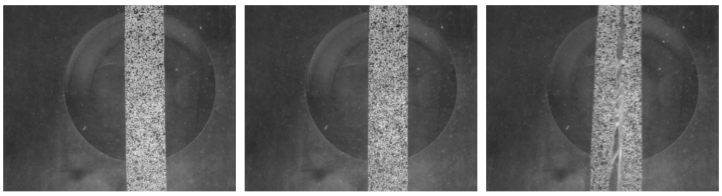

Figure 8. DIC Images, Tensile test at 60°C

while the adjacent lamina (90°) will tend to expand. This differential will lead to the bending of the cylinder, and has been exaggerated and represented in figure 7.

The values of axial stresses in figure 6*a* are the results of normal and bending stresses combined. It can be seen that bending-induced compressive stresses are superimposed on to existing tensile stress in the inner laminae of the cylinder. This compressive stress decreases in magnitude as we approach the middle of the wall, which acts as the neutral axis of the bent section. This explains the increasing tensile nature of stress in the first 0° and 90° laminae. Beyond the mid-wall position (or the neutral axis), the bending stresses become tensile in nature and increase in magnitude as one moves towards the outer surface. This manifests as the decreasing compressive stress in the second 90° lamina, and increasing tensile stress in the outermost 0° lamina. This variation of stress being linear with respect to radial position is akin to that of bending stresses versus distance from neutral axis.

4.3. Variations of parameters with temperature

A more accurate model is that which captures changes in material properties with temperature. The results of the tests described in section 4 have been plotted as shown in figure 9. Against each plot is the curve that describes the trend of variation. Although higher order polynomials may be used to more closely fit the values, they have not been used here as they deviate from realistic behaviour. The parameter ν_{23} was calculated using the expression given in [10].

The equations of variation, when used in the model developed, provide the variation of stresses and strains as shown in figure 10. The cylinder considered is of a $[0/90]_s$ layup with 4 laminae. Inner and outer radii are 6.35 and 6.858 mm respectively. The temperature varies linearly, between 120°C on the inner surface and 30°C on the outer surface.

Conclusion

Thus a methodology has been prescribed that facilitates the prediction of thermal stresses in composite cylinders, based on the assumptions that the temperature variation is radial and axisymmetric. The axisymmetric nature of the problem removes the need for analyzing shear effect. The study's verity was checked against the results of existing literature, and was utilized to check the effects of fiber/lamina orientation on the variation of stresses and strains along the radial direction of the cylinder. Finally, experimental results describing the variations of

(a)

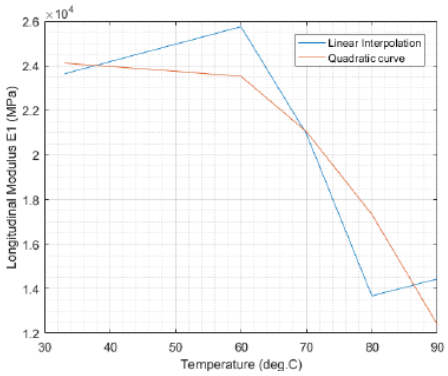

$E_1 = 1000*(-0.00613*T^2 + 0.5482*T + 12.71)$

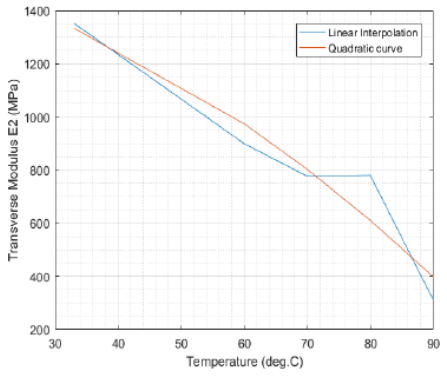

$E_2 = 1000*(-0.0001032*T^2 - 0.003723*T + 1.569)$

(b)

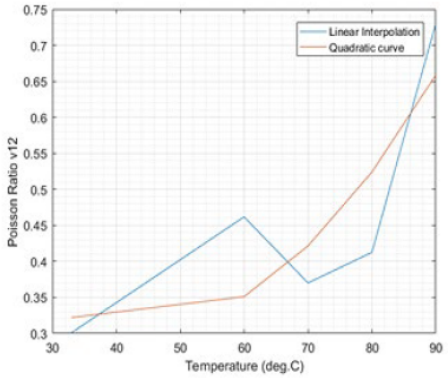

$\upsilon_{12} = 0.0001611*T^2 - 0.01391*T + 0.6057$

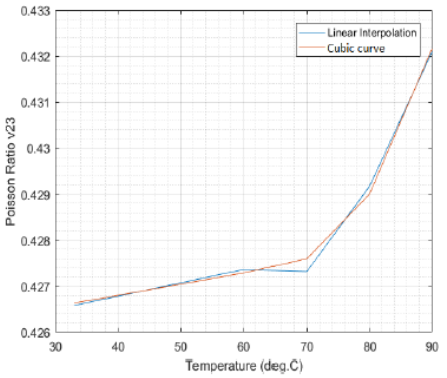

$\upsilon_{23} = 1.119e\text{-}7*T^3 - 1.805e\text{-}5*T^2 + 0.0009566*T + 0.4107$

(c)

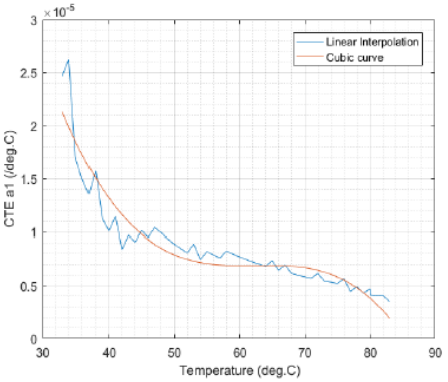

$\alpha_1 = -5.797e\text{-}10*T^3 + 1.084e\text{-}7*T^2 - 6.749e\text{-}6*T + 0.0001468$

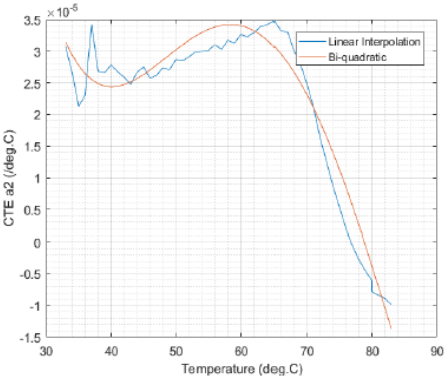

$\alpha_2 = 4.763e\text{-}11*T^4 - 1.259e\text{-}8*T^3 + 1.159e\text{-}6*T^2 - 4.45e\text{-}5*T + 0.0006338$

Figure 9. DIC Images, Tensile test at 60°C

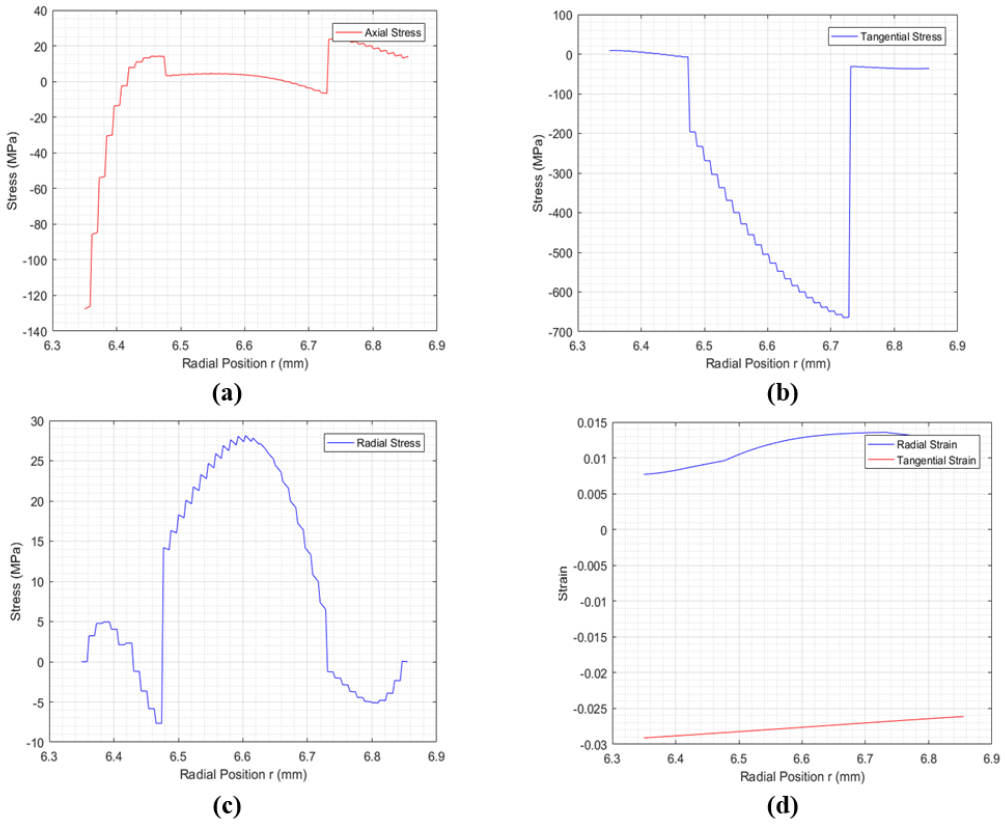

Figure 10. Variations of axial stress (a), hoop stress (b), radial stress (c), radial and hoop strains (d) in a $[0/90]_s$ layup

mechanical properties with temperature, were used in the model to obtain stresses and strains.

References

[1] Timoshenko S and Goodier J N 1951 *Theory of Elasticity* (New York, St. Louis, etc.: MacGraw Hill)
[2] Brischetto S and Carrera E 2009 Thermal stress analysis by refined multilayered composite shell theories *J. Therm. Stress* **32** (1-2) 165–86
[3] Raja Iyengar K T S and Chandrashekhara K 1966 Thermal stresses in a finite solid cylinder due to an axisymmetric temperature field at the end surface *Nucl. Engng Des.* **3** (1) 21–31
[4] Kari Thangaratnam R, Palaninathan, and Ramachandran J 1988 Thermal stress analysis of laminated composite plates and shells *Comput. Struct.* **30** (6) 1403–11
[5] Witherell M D 1992 A generalized plane-strain elastic stress solution for multiorthotropic-layered cylinder In *Technical Report AD-A250487, ARCCB-TR-92013, US Army Armament Research, Development and Engineering Center, Benet Laboratories* (New York)
[6] Witherell M D 1993 A thermal stress solution for multilayered composite cylinders In *Technical Report AD-A262579, ARCCB-TR-93005, US Army Armament Research, Development and Engineering Center, Benet Laboratories* (New York)
[7] Akcay I H and Kaynak I 2005 Analysis of multilayered composite cylinders under thermal loading *J. Reinf. Plast. Compos.* **24** (11) 1169–79
[8] Siegl M and Ehrlich I 2017 Transformation of the mechanical properties of fiber-reinforced plastic tubes from the cartesian coordinate system into the cylindrical coordinate system for the application of bending models *Athens J. Technol. Engng* **4** (1) 47–62
[9] Hyer M W, Cooper D E, and Cohen D 1986 Stresses and deformations in cross-ply composite tubes subjected to a uniform temperature change *J. Therm. Stress* **9** (2) 97–117
[10] Foye R L 1972 The transverse Poisson's ratio of composites *J. Compos. Mater.* **6** (2) 293–5